Bioorganic & Medicinal Chemistry 19 (2011) 5291–5299

Contents lists available at SciVerse ScienceDirect

Bioorganic & Medicinal Chemistry

journal homepage: www.elsevier.com/locate/bmc

# Synthesis, structural, and biological evaluation of bis-heteroarylmaleimides and bis-heterofused imides

Nicola Ferri [b], Tiziano Radice [a], Manuela Antonino [b], Egle Maria Beccalli [a], Stella Tinelli [c], Franco Zunino [c], Alberto Corsini [b], Graziella Pratesi [c], Enzio M. Ragg [d], Maria Luisa Gelmi [a], Alessandro Contini [a,*]

[a] Dipartimento di Scienze Molecolari Applicate ai Biosistemi – Sezione di Chimica Organica "A. Marchesini", Università degli Studi di Milano, Via Venezian 21, 20133 Milano, Italy
[b] Dipartimento di Scienze Farmacologiche, Università degli Studi di Milano, Via Balzaretti 9, 20133 Milano, Italy
[c] Fondazione IRCCS Istituto Nazionale Tumori, Via Venezian 1, 20133 Milano, Italy
[d] Dipartimento di Scienze Molecolari Agroalimentari – Sezione di Chimica Organica, Università degli Studi di Milano, Via Celoria 2, 20133 Milano, Italy

ARTICLE INFO

*Article history:*
Received 27 June 2011
Revised 28 July 2011
Accepted 9 August 2011
Available online 16 August 2011

*Keywords:*
DNA intercalator
Microwave chemistry
NMR spectroscopy
Molecular dynamics
Biological activity

ABSTRACT

Bis-2,3-heteroarylmaleimides and polyheterocondensed imides joined through nitrogen atoms of the *N,N'*-bis(ethyl)-1,3-propanediamine linker were prepared from substituted maleic anhydrides and symmetrical diamines in good to satisfactory yields and short reaction times using microwave heating. The novel molecules were shown to inhibit proliferation of human tumor cells (NCI-H460 lung carcinoma) and rat aortic smooth muscle cells (SMCs) with variable potencies. Compound **11a**, the most potent one of the series, showed $IC_{50}$ values comparable to those observed for the leading molecule elinafide in both cell lines, but with a higher selectivity toward human tumor cells. Compound **11a** affected G1/S phase transition of the cell cycle, showed in vitro DNA intercalating activity and in vivo antitumor activity. A thorough structural analysis of the **11a**-DNA complex was also made by mean of NMR and computational techniques.



## 1. Introduction

Several examples of bis-intercalator agents, whose typical features are the presence of two identical (i.e., naphthalimide,[1–7] benzonaphthalimide,[8] imidazoacridanone,[9,10] antracyclinone,[11,12] acridinecarboxamide,[13] phenazinecarboxamide,[14,15] rebeccamycin,[16] and anthrapyrazole,[17] rings) or dissimilar chromofores[18,19] connected by a flexible chain containing nitrogen atoms, are reported in the literature. Studies related to the features of the chain, both concerning length and structural constraints, are also reported.[8,14,20] Furthermore, SAR studies were reported by Braña et al. on elinafide analogs containing aromatic fused heterocycles,[21–25] aryl or heteroaryl substituted elinafides as well as their aza-analogs.[26] More recently, we reported the biological activity of a series of molecules belonging to the classes of 2,3-heteroaryl substituted maleimides of kind **1** and heterofused imides of kind **2** (Fig. 1), characterized by heteroatom and $\pi$-system extension diversity, against human tumor cells (NCI-H460 lung carcinoma) and rat aortic smooth muscle cells (SMCs).[27]

The antiproliferative profile of some of the above compounds is comparable to the one of amonafide (**3**, Fig. 2) which is classified as a mono-intercalator of DNA.

The antitumor activity of **3** seems to be related to its ability to stabilize the DNA-intercalator-topoisomerase II ternary complex 1. By contrast, its parent elinafide (**4**, Fig. 2) and its derivatives are potent bis-intercalator of DNA[1–5] and do not stabilize the topo II-DNA complex.[25,26] DNA intercalation assays on selected compounds of series **2** showed that, in contrast to **4**, they do not directly interact with DNA.[27]

As documented by the literature, the preparation of dimeric compounds represents an attractive strategy to increase both

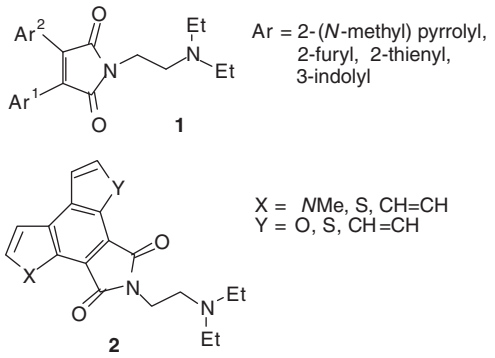


**Figure 1.** 2,3-Heteroaryl maleimides **1** and heterofused imides **2**.

* Corresponding author. Tel.: +39 02 503 14480; fax: +39 02 503 14476.
*E-mail address:* alessandro.contini@unimi.it (A. Contini).

0968-0896/$ - see front matter © 2011 Elsevier Ltd. All rights reserved.
doi:10.1016/j.bmc.2011.08.016

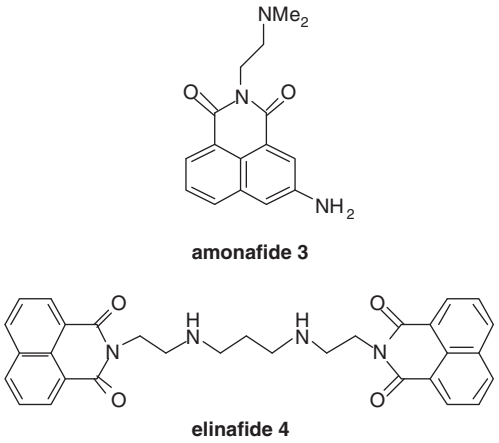


**Figure 2.** DNA-interacting compounds.

DNA binding affinities and selectivity. In this study, we report the synthesis, the antiproliferative activity and the DNA intercalation of new bis-intercalator agents belonging to the classes of 2,3-heteroaryl substituted maleimides and heterofused imides using, as the linker, the *N*,*N*′-bis-(2-aminoethyl)-1,3-propanediamine which is generally considered the most suited one, as demonstrated by several studies.[8,14] In analogy with our previous study,[27] the human NCI-H460 lung carcinoma cell line and a rat aortic SMC cell line were used due to the interest of DNA-intercalating agents in the therapy of tumor as well as in cardiovascular diseases. Compound **11a** was selected as the most potent one, eliciting antiproliferative effects comparable to those of **4** on both cell types. This compound was shown to directly interact with DNA in vitro and to inhibit cellular proliferation by interfering with the progression of G1/S phase of the cell cycle. Moreover, in human NCI-H460 tumor xenografts it was shown to reduce tumor growth in a dose-dependent manner.

## 2. Chemistry

The preparation of compounds **7** took advantage of a very efficient procedure consisting in the use of microwave heating (Scheme 1).

Compounds **7a–d**, **f**, and **g** were prepared in good yields (40–98%) from the anhydrides **5a–d**, **f**, and **g** and *N*,*N*′-bis-(2-aminoethyl)-1,3-propanediamine **6** operating in $CH_2Cl_2$ at 100 °C and 450 W in 15 min. Instead, the preparation of **7e** (30%) and **7h** (82%) from the corresponding anhydrides **5e** and **5f** and diamine **6** required DMF as the solvent and microwave heating at 450 W and 130 °C (5 min). The reaction between the anhydride **5c** and the amine **8** gave compound **9** in quantitative yield ($CH_2Cl_2$, 100 °C, 450 W, 15 min).

As preliminary biological assays revealed that **7a**, **d**, and **h** were the most promising moieties (see Table 1), the preparation of corresponding bis-heterofused imides **11a–c** was planned. Starting from **10a** and **b** and using traditional heating the reaction was unsuccessful and a mixture of compounds, not isolable in pure form, was formed. On the other hand, satisfactory results were achieved by making **10a** to react with **6** in DMF using microwave (450 W) at 100 °C. Compound **11a** was obtained after 15 min and was isolated in pure form in 60% yield (Scheme 2).

The microwave assisted reaction (15 min) was also performed starting from **10b** (600 W, 120 °C) and **10c** (450 W, 130 °C) providing compounds **11b** (24%) and **11c** (65%), respectively.

## 3. Biological evaluation

The antiproliferative effect of compounds of the series **7**, **9**, and **11** was evaluated, after three days of exposure, in cultured rat aortic SMCs and in human NCI-H460 lung tumor cell lines (Table 1).

The $IC_{50}$ values for the novel molecules ranged from 0.09 to more than 30 μM in SMCs, and from 0.003 to more than 30 μM in the tumor cell line. Within compounds **7**, characterized by the presence of two heteroaryl substituents on the maleimide ring, compound **7a** was found moderately potent in both cell lines, while **7d** and **h** were the most effective on NCIH-460 and SMCs, respectively. Instead, within the polyheterocondensed imides **11**, compound **11a** had potency levels comparable to those of **4**, while the others proved to be less potent. Importantly, compound **11a** decreased cell proliferation of the tumor cell line with an $IC_{50}$ value 30-fold lower than that calculated for rat SMCs, that is, 0.003 μM versus 0.09 μM, respectively, while compound **11b**, although less potent than **11a**, showed an even more selective antiproliferative effect with an about 500-fold preference toward the human tumor cell line (Table 1). It should be noted that, in the same experimental conditions, the reference compound **4** showed a really modest selectivity (1.5-fold) toward the NCIH-460 line.

It should also be noted that, for compounds **11a** and **b**, dimerization using an amine-type linker of the proper length and physicochemical properties has a dramatic influence on the biological activity. Indeed, the corresponding *N*-diethylamminoethyl substituted monomers **2**, previously reported as compound **12a** (X = NMe, Y = O, $IC_{50}$ = 5.3 and 8.6 μM on SMC and NCI-H460, respectively) and **12d** (X = S, Y = O, $IC_{50}$ >30μM on both cell lines),[27] in the same experimental conditions showed a potency

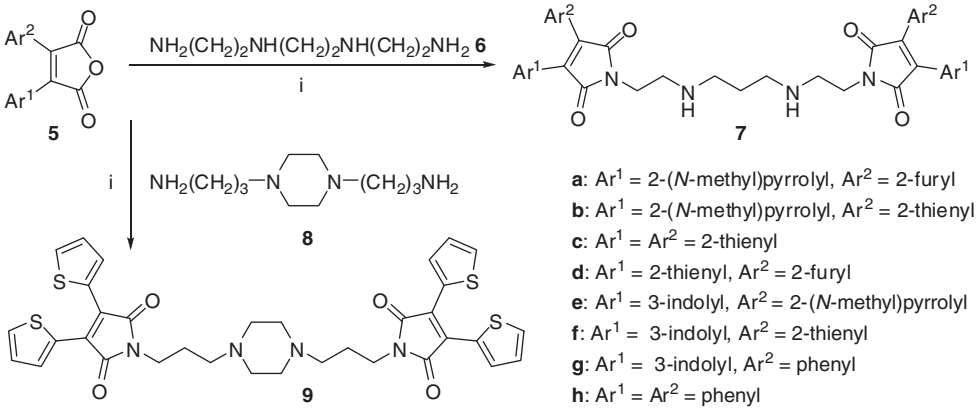


**Scheme 1.** Synthesis of bis-2,3-heteroaryl maleimides **7** and **9**. Reagents and conditions: (i) **7a–d**,**f**,**g**, **9**: $CH_2Cl_2$, Mw (450 W, 100 °C); (ii) **7e**,**h**: DMF, Mw (450 W, 130 °C).

**Table 1**
Antiproliferative effects of compounds **7**, **9** and **11** in rat aortic SMCs and human tumor cell line NCI-H460

| Compd. | Imide moiety | $IC_{50}$ (μM) SMCs | $IC_{50}$ (μM) NCIH-460 |
|---|---|---|---|
| **4** | 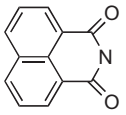 | 0.012 | 0.008 |
| **7a** | 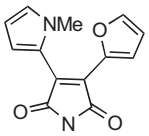 | 0.73 | 0.65 |
| **7b** | 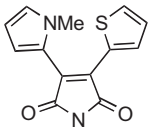 | 1.8 | 3.4 |
| **7c** | 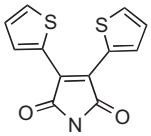 | 1.3 | 4.3 |
| **7d** | 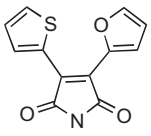 | 3.5 | 0.5 |
| **7e** | 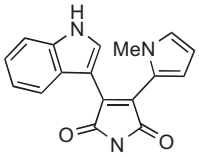 | 16.5 | 3.9 |
| **7f** | 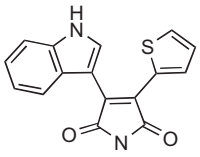 | 4.7 | 4.2 |
| **7g** | 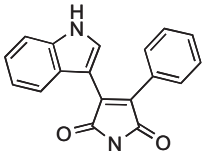 | 1.0 | 3.9 |
| **7h** | 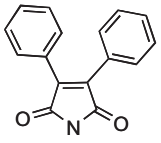 | 0.62 | 1.2 |
| **9** | 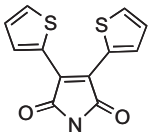 | >30 | >30 |
| **11a** | 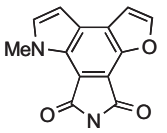 | 0.09 | 0.003 |
| **11b** | 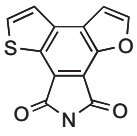 | >30 | 0.07 |

**Table 1** (*continued*)

| Compd. | Imide moiety | $IC_{50}$ (μM) SMCs | $IC_{50}$ (μM) NCIH-460 |
|---|---|---|---|
| **11c** | 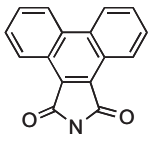 | 0.23 | 0.4 |

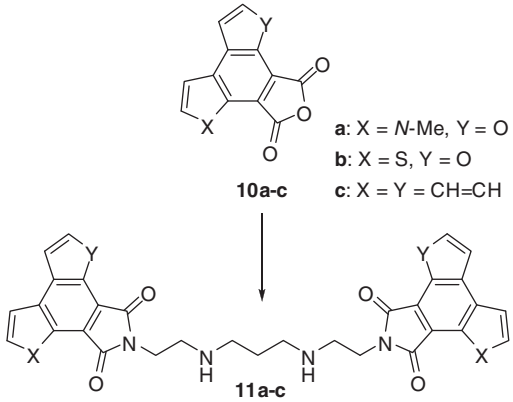


**Scheme 2.** Synthesis of bis-heterofused imides **11**. Reagents and conditions: (i) DMF, Mw (**10a**: 450 W, 100 °C, **10b**: 600 W, 120 °C; **10c**: 450 W, 130 °C).

**Table 2**
Effect of compound **11a** on cell cycle of human NCI-H460 cells

| Incubation | G0/G1 (%) | S (%) | G2/M (%) |
|---|---|---|---|
| 0.4% FCS | 64.25 ± 0.68 | 11.17 ± 1.16 | 24.59 ± 1.84 |
| 10% FCS | 54.39 ± 2.0 | 20.51 ± 0.14 | 25.10 ± 1.85 |
| 10% FCS + **11a** | 76.63 ± 1.62 | 10.56 ± 1.79 | 12.81 ± 0.16 |
| 10% FCS + **4** | 68.40 ± 1.582.0 | 13.44 ± 1.56 | 18.15 ± 0.02 |

Results are representative of three replicate experiments.

from about 100 to about 3000-folds lower than the dimers. Curiously, the same ratio was not observed for compound **11c**, where the corresponding monomer (**12i**, in Ref. 27) resulted almost equally potent ($IC_{50}$ = 0.68 and 0.9 μM on SMC and NCI-H460, respectively).

To further investigate the antiproliferative mechanism of action of compound **11a**, we analyzed the cell cycle progression of human NCI-H460 cells by flow cytometry analysis. Incubation of NCI-H460 cells with 0.4% FCS led to accumulation of cells at G0/G1 phase (64.25 ± 0.68%) with only a small percentage at S phase (11.17 ± 1.16%). After incubation for 20 h with 10% FCS we observed a significant increase in the proportion of NCI-H460 cells in S phase (20.51 ± 0.14%), which was decreased to 13.44 ± 1.56% by 0.08 μM of **4** and to 10.56 ± 1.791% by 0.003 μM of compound **11a** (Table 2).

Importantly, we did not observe a significant increase in the percentage of cells at sub-G0/G1 phase, demonstrating a specific antiproliferative activity of both **4** and **11a**, without induction of apoptosis (Fig. 3).

With the aim to evaluate if the antiproliferative effect of compound **11a** was a consequence of DNA intercalation or an inhibitory action on the DNA topoisomerase II activity, we performed an in vitro DNA topoisomerase II activity assay (Fig. 4). Incubation of compounds **11a** and **4**, at concentrations of 0.1 μM, with plasmid DNA in the presence of DNA topoisomerase II altered the DNA electrophoretic mobility on agarose gel, indicating a possible inhibitory

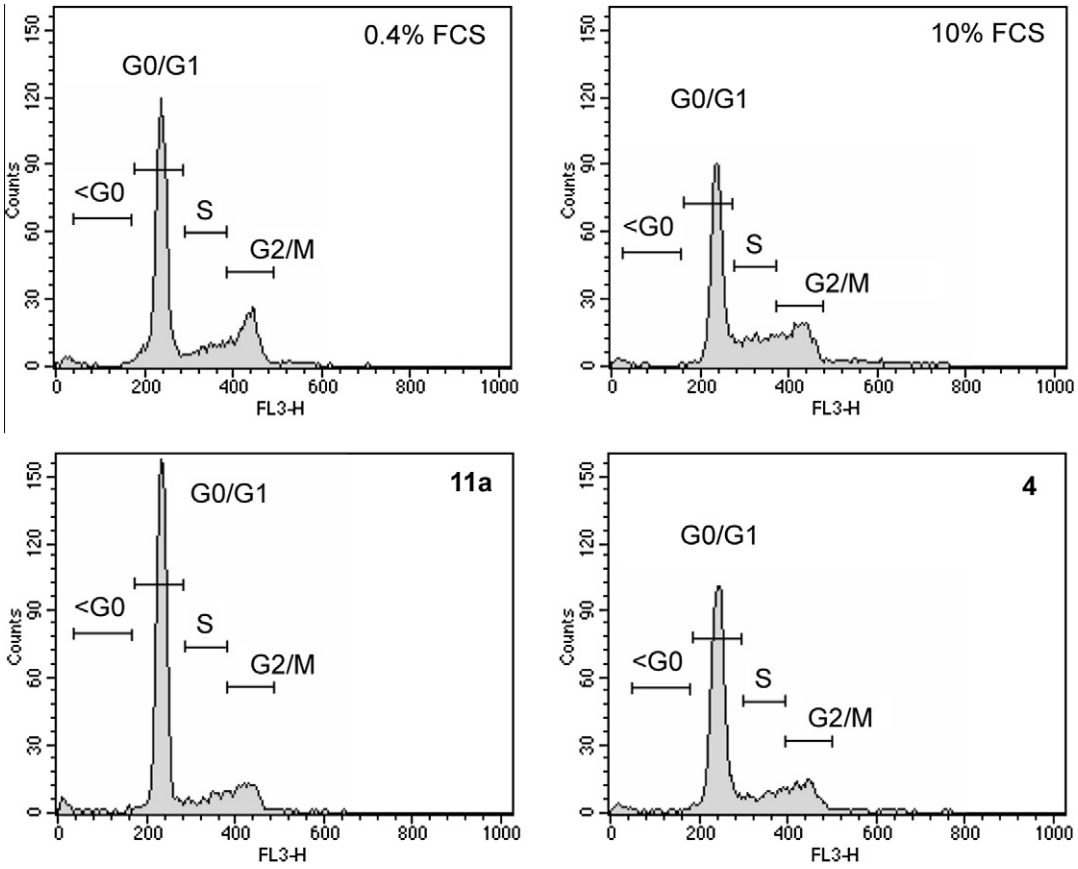


**Figure 3.** Effect of compounds **4** and **11a** on cell cycle progression of human NCI-H460 cells. Cells were seeded at a density of $2 \times 10^5$ per 35-mm dish and incubated with RPMI supplemented with 10% FCS. Twenty-four hours later, the medium was changed with medium containing 0.4% FCS to stop cell growth, and the cultures were incubated for 2 days. At this time, the medium was replaced with medium containing 10% FCS, in the presence or absence of compound **4** (0.08 μM) or compound **11a** (0.003 μM). After 18 h, at 37 °C, cell cycle analysis was performed by FACS. The results are representative of three independent experiments conducted in duplicate.

effect on topoisomerase II (Fig. 4A). However, a similar shift of the DNA electrophoretic mobility was also observed in the absence of the topoisomerase II, suggesting that both compounds efficiently interacted with plasmid DNA (Fig. 4B). These results indicated that the bis-intercalating agent **4** as well as compound **11a** did not affect the activity of the DNA topoisomerase II, but elicited their antiproliferative action through a direct interaction to DNA.

Compound **11a** was selected for in vivo testing and antitumor activity evaluation, due to its high potency against the NCI-H460 tumor cell line. Tumor fragments were implanted by sc injection in both flanks of nude athymic mice. The compound was administered iv, from day 2, every 4th day for four times (q4dx4). Control mice received vehicle alone (DMSO 10% in water). Due to the low solubility of the molecule, the higher dose tested was 16.9 mg/kg, which resulted active ($P$ <0.01 vs controls) and well tolerated. A clear dose–response was observed in the antitumor effect of the compound, since the lower dose tested was unable to significantly inhibit tumor growth (Fig. 5).

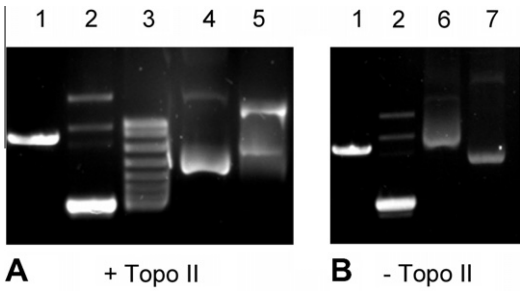


**Figure 4.** Effect of **4** and **11a** on DNA topoisomerase II activity. (1) Linear pRYG DNA; (2) Supercoiled pRYG DNA; (3) pRYG DNA + Topo II; (4) pRYG DNA + Topo II + **4**; (5) pRYG DNA + Topo II + **11a**; (6) pRYG DNA + **4**; (7) pRYG DNA + **11a**.

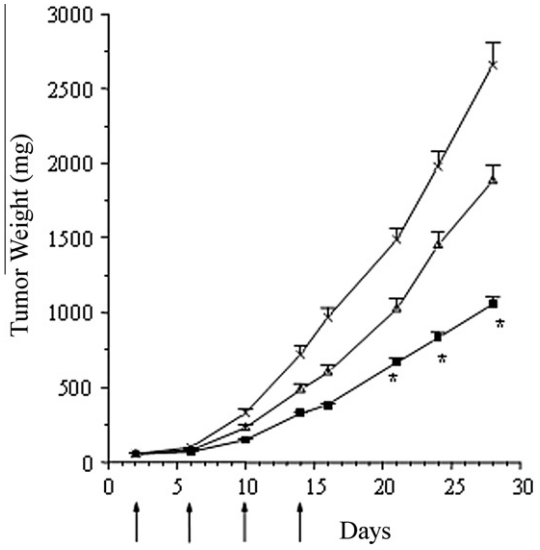


**Figure 5.** Antitumor activity for compound **11a** on human NCI-H460 lung tumor xenograft. Tumors were generated by *s.c.* implant of fragment in both flanks of athymic nude mice. Mice were treated i.v. at days 2, 6, 10, and 14 (arrows) with: solvent (X); compound, 10 mg/Kg (▲) or 16.9 mg/Kg (■). Mean tumor weight of 8 mice/group are shown. Bars: Standard errors. *$P$ <0.01 by Student's $t$-test.

## 4. Structural evaluation of the DNA-11a complex

In order to further characterize the binding properties of **11a** to DNA, the self-complementary oligodeoxynucleotide d(CGGCCG)$_2$ was chosen as model, on the basis of previous DNA foot-printing studies pointing out the preference for CG-rich sequences of bis-naphthalimides.[24,25]

The $^1$H NMR spectrum of **11a-**trifluoroacetate, dissolved in $D_2O$, is characterized by a general line-broadening and a high-field shift by approximately 1.5 ppm, with respect to the free base, of the aromatic proton resonances, a clear indication of extensive self-aggregation. When the hexanucleotide d(CGGCCG)$_2$ is added to the **11a-**trifluoroacetate solution an even more pronounced loss of resolution is observed, at low DNA/drug ratios, due to the formation of high molecular weight aggregates. This is mainly caused by the polyelectrolyte nature of DNA, which initially favors nonspecific external binding of the ligand. However, at DNA/drug values greater than 0.25, new sharp and well resolved resonances appear with increasing intensity until a unitary molar ratio is reached, thus suggesting the formation of one or more well-defined complexes when DNA and ligand are present at comparable concentrations (see Fig. S1, Supplementary data).

In principle, four different orientations of **11a** could be devised for its intercalation into the hexanucleotide, of which only two maintain the overall $C_2$-symmetry of the complex (i.e., those with the two aromatic moieties in antiparallel orientation, see Figure 6A and C) while the other two (those with the aromatic systems in parallel orientation, Figure 6B), destroy the inherent molecular symmetry and give rise to intrinsically different chemical environments for each proton residing on DNA strands and ligand.

As a result, a resonance splitting would be expected for hydrogen atoms residing in close proximity of the binding site. Indeed, such splitting was observed especially when cooling the solution below room temperature, thus proving the existence of several exchange equilibria involving more than one complex with a rate comparable to the NMR time-scale. An example of such splitting is shown in Figure 7, which depicts sections of a 2D-NOESY experiment performed at 15 °C on a 1:1 complex of **11a**-trifluoroacetate with 5′-d(CGGCCG)$_2$-3′.

For the sake of clarity, oligonucleotide residues have separately been numbered as follows: 5′-d($C_1G_2G_3C_4C_5G_6$)-3′/5′-d($C_7G_8G_9C_{10}C_{11}G_{12}$)-3′, while ligand protons have been numbered following IUPAC rules (labels ‘a’ and ‘b’ refer to the two aromatic moieties, becoming magnetically nonequivalent in the case of a nonsymmetric complex). The 2D-NOESY spectrum (see also Fig. S2,Supplementary data, for details) actually displays three kinds of correlations: (a) intra-residue NOE interactions involving protons that reside either on DNA or on ligand moieties (continuous lines); (b) intermolecular NOEs involving proton pairs residing on both ligand and DNA (continuous lines); and (c) cross-peaks due to chemical exchange of the various orientations of ligand within DNA (dotted lines). Examples of some significant intra-molecular interactions for the complete assignment of the ligand aromatic protons, as well as their intermolecular NOE interactions are also reported in Figure 7 (Chemical shift assignments are listed in Table S1, Supplementary data). Particularly meaningful are the two well separated resonances at 3.17 and 3.58 ppm, attributed to the methyl groups (**11a**-6Ha and **11a**-6Hb) residing on the ligand pyrrolyl moieties. Each methyl group displays intra-residue NOE interactions with the protons at adjacent positions (**11a-**5Ha and 5Hb at $\delta$ 7.0 and 6.35 ppm, respectively), as well as strong intermolecular NOEs, respectively, with $G_2$,$G_3$-1′H and $C_{10}$,$C_{11}$-5H. These base-pairs define an intercalation site constituted by the $G_2G_3/C_{10}C_{11}$ DNA region. Due to the self-complementarity of the hexanucleotide, a second intercalation site is defined by the symmetry related segment $C_4C_5/G_8G_9$.

The splitting observed for both ligand and DNA $^1$H resonances clearly indicates that two main complexes exist in solution, differing only by the orientation of the ligand aromatic moiety, which always intercalates between the $G_2$:$C_{11}$ and $G_3$:$C_{10}$ base pairs. The first orientation (orientation A) is defined by the pyrrolyl and furanyl moieties interacting respectively with $G_2G_3$ and $C_{10}C_{11}$ residues of DNA, whereas the second one (orientation B) involves the pyrrolyl moiety interacting with $C_{10}C_{11}$ residues (see Fig. 6). These two orientations are present in solution in equal amounts, as indicated by the respective resonance intensities measured in the 1D-NMR spectra (see Fig. 7 on top).

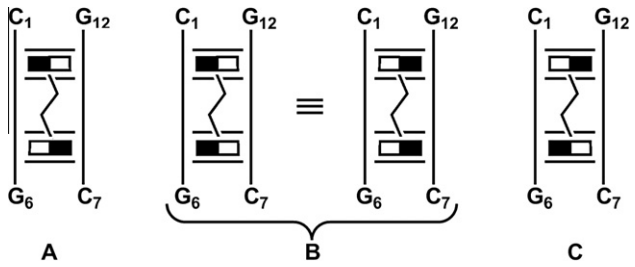


**Figure 6.** Possible binding orientations of compound **11a** intercalated into d(CGGCCG)$_2$.

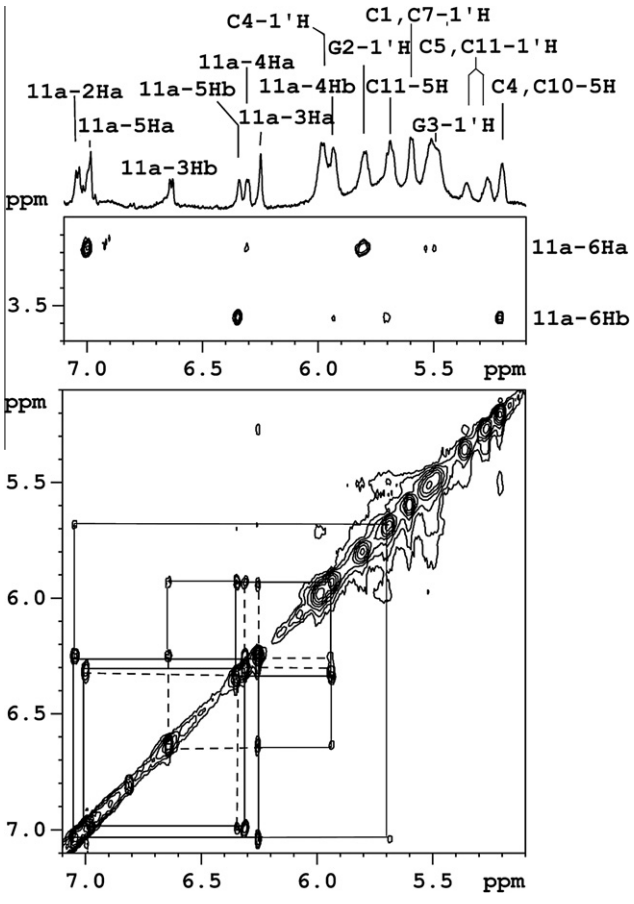


**Figure 7.** Expansion of the 2D-NOESY spectrum (low-field and methyl regions) performed on the **11a**-trifluoroacetate:d(CGGCCG)$_2$ complex in $D_2O$ ($3 \times 10^{-4}$ M, NaCl $25 \times 10^{-3}$ M, pH 5.5) at 15 °C, $t_{mix}$ = 0.24 s. Continuous lines: inter- and intra-molecular NOEs; dotted lines: cross-peaks due to chemical exchange. The corresponding 1D-spectrum is shown on top, together with the most significant resonance assignments.

**Table 3**
Experimental[a] (**$d^{exp}$**), calculated[b] NOE distances (**<$d^{calc}$>**) and errors[c] (**err**).derived for **11a** intercalated into d(CGGCCG)$_2$ major and minor grooves (orientation B). All values are given in Å

| Proton pair | | $d^{exp}$ | <$d^{calc}$> (major) | err (major) | <$d^{calc}$> (minor) | err (minor) |
|---|---|---|---|---|---|---|
| i | j | | | | | |
| G2–H1′ | H6a | 2.5 | 2.7 | −0.2 | 3.0 | −0.5 |
| G3–H8 | H6a | 3.6 | 4.1 | −0.5 | 5.7 | −2.1 |
| C4–H1′ | H6b | 4.1 | 5.0 | −0.9 | 4.2 | −0.1 |
| C4–2H2′ | H5b | 3.7 | 2.9 | 0.8 | 6.3 | −2.6 |
| C4–1H2′ | H5b | 3.0 | 3.0 | 0.0 | 5.7 | −2.7 |
| C4–H5 | H6b | 2.9 | 3.6 | −0.7 | 4.1 | −1.2 |
| C5–H5 | H5b | 3.9 | 4.6 | −0.7 | 4.6 | −0.7 |
| C5–H5 | H6b | 3.5 | 3.8 | −0.3 | 3.9 | −0.5 |
| C10–H1′ | H3a | 3.0 | 4.0 | −1.0 | 8.7 | −5.7 |
| C10–1H2′ | H3a | 2.9 | 3.2 | −0.3 | 8.2 | −5.3 |
| C10–1H2′ | H2a | 2.6 | 2.8 | −0.1 | 5.9 | −3.2 |
| C10–2H2′ | H2a | 3.1 | 3.2 | −0.1 | 6.5 | −3.4 |
| C10–2H2′ | H3a | 3.2 | 2.9 | 0.3 | 8.5 | −5.3 |
| C10–H6 | H2a | 2.8 | 3.6 | −0.8 | 5.3 | −2.4 |
| C10–H5 | H2a | 4.0 | 3.9 | 0.0 | 3.9 | 0.1 |
| C11–H1′ | H3a | 2.9 | 3.7 | −0.8 | 10.6 | −7.6 |
| C11–H5 | H2a | 3.0 | 3.4 | −0.3 | 5.8 | −2.8 |
| C11–H5 | H3a | 3.2 | 4.4 | −1.2 | 8.1 | −4.9 |
| C11–H6 | H2a | 2.8 | 3.7 | −0.8 | 7.9 | −5.0 |
| H2a | H3a | 2.7 | 2.8 | −0.1 | 2.7 | −0.1 |
| H3a | H4a | 3.1 | 2.8 | 0.3 | 2.8 | 0.3 |
| C5–H5 | C5–H6 | 2.4 | 2.4 | 0.0 | 2.4 | 0.0 |
| St. deviation | | | | 0.5 | | 2.2 |

[a] Interproton distances derived from experimental 2D-NOESY cross-peak volumes by applying the following equation $d_{ij} = d_{ref} \times (V_{ref}/V_{ij})^{1/6}$, where $d_{ref}$ and $V_{ref}$ refer to proton pairs at fixed distance chosen as reference.
[b] theoretical distances calculated as averages from the 8 ns production MD run with the following equation: $d^{calc} = (\sum_{i=1,N} d_i^{-6})^{-1/6}/N$.
[c] err = ($d^{exp} - d^{calc}$).

This corresponds to a 180° flip of the ligand aromatic system within the intercalation site, occurring on a relatively long timescale, with rates estimated about 0.7 $s^{-1}$ on the basis of the exchange cross-peak volumes measured at 15 °C. This value is in line with that one reported for the bulkiest derivatives of compound **4**.[28,29] Thus, compound **11a** is likely to behave as other known bis-imide intercalators that were shown to be major groove binders.[21,28]

In order to fully ascertain whether **11a** is a major- or a minor-groove binder, a quantitative analysis of NOE-based inter-proton distances was necessary, supported by molecular modeling and independent molecular dynamics (MD) calculations. Structures of compound **11a** in the three orientations A, B, and C intercalated in either the major and minor groove were built and subjected to an unrestrained molecular dynamics run with the explicit inclusion of water molecules as solvent. After proper equilibration, an 8 ns simulation run was produced and the trajectories were processed using the MM-PBSA approach, which in previous studies was shown to be able to discriminate binding conformations on an energetic basis with an error between 1.5 and 2.5 kcal/mol, on the average.[30,31] The computed binding free energy differences showed a moderate preference for the major groove conformations ($\Delta G$: −49.5 vs −48.5 kcal/mol, as the average among A, B, and C conformations), but energy differences resulted well below the accuracy limits of the method (Table S2, Supplementary data).

Aiming to discriminate between major and minor groove binding preferences, theoretical NOE distances were calculated from MD trajectories and compared to experimental NOE distances. Calculated distances, averaged from orientation B over the whole 8 ns trajectory, are reported in Table 3.

Orientation B was chosen as the most representative of all the possible local orientations, but comparable results were obtained also by performing the same distance analysis on orientations A and C. Theoretical values obtained for the major groove complex fit particularly well with experimental NOE distances, while significant deviations were obtained for the minor groove complex (SD: 0.5 and 2.2 Å, respectively). It should be noted that MD simulations were carried out without any experimentally derived restraint, thus giving support to the validity of the adopted protocol.

In conclusion, those results, obtained from NMR experiments and theoretical calculations, indicate that compound **11a** is able to bis-intercalate at the level of the major groove in two possible and energetically equivalent binding modes, which only differ in the orientation of the heterocyclic moiety within the intercalation site and equilibrate in solution, probably through the (slow) formation of a mono-intercalated intermediate (see Scheme 3).

Such molecular intermediate escaped NMR detection, but its concentration must necessarily be very low. In the case of elinafide:d(ATGCAT)$_2$ complex, an alternative ring-flip mechanism has also been proposed, involving internal rotation within the intercalation site.[29] As this alternative motion should be linked with the opening and closing of external base-pairs, a motion that certainly occurs in the less stable A:T base-pairs at terminal positions, we feel that in our case the 'slide-out and ring-flip' mechanism is more likely to occur, given the 'CG-rich' character of our oligonucleotide and the increased diameter of the aromatic moiety in **11a**, with respect to elinafide and the tested derivatives.

Hydrogen bond analysis revealed that the bis-intercalated complexes are well stabilized by two hydrogen bonds between the protonated amino groups of the linker chain and the carbonyl groups of $G_3$ and $G_9$ facing the major groove, as shown in Figure 8.

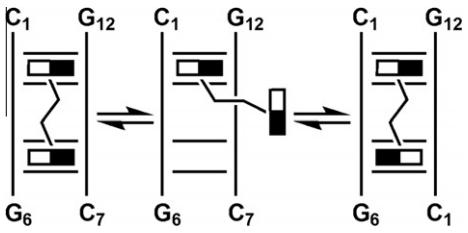


**Scheme 3.** The "slide-out and ring-flip" mechanism.

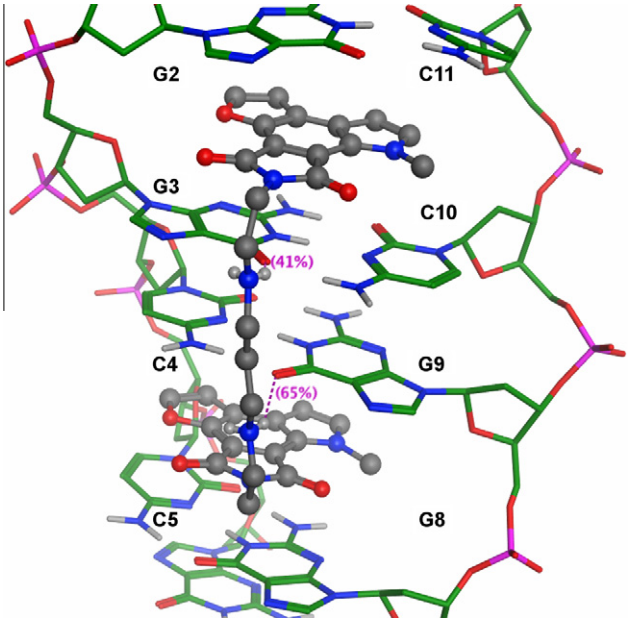


**Figure 8.** Geometry of **11a** bis-intercalated into DNA (orientation B) obtained by averaging 8000 frames extracted from the 8 ns MD simulation (rotation and translations were removed before averaging). H-bonds are reported as dotted lines, together with their average population (%).

Although in complex with DNA, the ligand undergoes significant internal motions, as both the aromatic moiety and the linker chain independently reorient themselves within a two-state jump model (see Fig. S4, Supplementary data).

## 5. Conclusion

In conclusion, new bis-2,3-heteroarylmaleimides **7** and polyheterocondensed imides **11** jointed through nitrogen atoms of the *N,N′*-bis(ethyl)-1,3-propanediamine linker were prepared and their ability to inhibit in vitro the proliferation of human tumor cells (NCI-H460 lung carcinoma) and rat aortic smooth muscle cells (SMCs) was evaluated. **11a** resulted the most potent compound of the series and showed to be selective for the NCIH-460 line, with an $IC_{50}$ value 30-fold lower than that calculated for rat SMCs, (i.e., 0.003 μM versus 0.09 μM, respectively). In terms of potency, **11a** is comparable to the lead compound **4** in both cell lines, but for this latter a really modest selectivity (1.5-fold) toward the tumor cell line was observed. The parent compound **11b**, although less potent than **11a**, showed an even more selective antiproliferative effect with an about 500-fold preference toward the human tumor cell line. The antitumor activity of compound **11a** was also demonstrated by in vivo studies in mice on human NCI-H460 lung tumor xenograft. Finally, a thorough structural analysis of the **11a**-DNA complex was also made by means of NMR and computational techniques. The DNA intercalating ability of bis-2,3-heteroarylmaleimides, initially observed through in vitro assays, was thus confirmed also providing useful insights into the dynamic behavior of the complex which might lead to further structural optimization of this class of bis-intercalators.

## 6. Experimental

### 6.1. Chemistry

Compounds **5a**,**b**,**d**,**e**,**f**,**g**,[32] **5c**,[27] **10a**,**b**[27] and **10c**[33] were prepared according to known procedures. Compound **5h** is a commercial available compound.

#### 6.1.1. General procedure for the preparation of bis-maleimides 7a–d,f,g and 9

Amine **6** (0.025 mL, 0.15 mmol) or **8** (0.031 mL, 0.15 mmol) was added to a solution of anhydride **5** (0.3 mmol) in $CH_2Cl_2$ (3 mL). The mixture was stirred under microwave heating (100 °C, 450 W) in the presence of a Weflon stirrer (**7a–d,f,g, 9**: 15 min). The mixture was cooled at room temperature and water (5 mL) was added. The organic layer was separated, dried over anhydrous $Na_2SO_4$ and filtered. The solvent was evaporated and the residue was purified by crystallization. In case of **5g**, a solid was formed during the reaction which was filtered from the hot solution, washed with $CH_2Cl_2$ to give pure compound **7g**. Pure compound **9** was directly obtained from the reaction mixture by addition of $Et_2O$ and washing the solid with the same solvent.

#### 6.1.2. General procedure for the preparation of 7e,h

*N,N′*-Bis-(2-Aminoethyl)-1,3-propanediamine (**6**) (0.03 mL, 0.17 mmol) and anhydride **5e** or **h** (0.34 mmol) were dissolved in DMF (8 mL). The mixture was stirred under microwave heating (130 °C, 450 W) in the presence of a Weflon stirrer for 5 min. The mixture was cooled at room temperature and diluted with a solvent (**5e**: AcOEt, 15 mL; **5h**: $Et_2O$, 15 mL) and brine (10 mL). The organic layer was separated, washed with water, dried over anhydrous $Na_2SO_4$ and filtered. Pure compound **7e** was obtained after crystallization. Instead, when the ethereal solution was concenterd, a yellow solid was separated corresponding to pure **7h**.

#### 6.1.3. General procedure for the preparation of compounds 11a–c

To a solution of anhydride **10** (0.39 mmol) in DMF (6 mL), was added *N,N′*-bis(2-aminoethyl)-1,3-propanediamine **6** (0.033 mL, 0.19 mmol). The mixture was stirred under microwave heating (**10a**: 450 W, 100 °C; 1**0b**: 600 W, 120 °C; **10c**: 450 W, 130 °C) for 15 min. Starting from **10a,b**, the mixture was then diluted with $Et_2O$ (15 mL) and brine (10 mL). A solid was formed, filtered and washed with $Et_2O$ to give pure compounds **11a,b**. Starting from **10c**, a solid was directly formed in the reaction mixture which was collected and washed with $Et_2O$ affording pure **11c**.

### 6.2. Biological methods

#### 6.2.1. Cell culture

The human NCI-H460 lung tumor cells and primary rat aortic SMCs were used in this study. SMCs cultured from the intimal-medial layers of aorta of male Sprague–Dawley rats (200–250 g) were grown in monolayers at 37 °C in a humidified atmosphere of 5% $CO_2$ in DMEM supplemented with 10% (v/v) fetal calf serum (FCS), 100 U/ml penicillin, 0.1 mg/mL streptomycin, 20 mM tricine buffer, and 1% (v/v) non-essential amino acid solution. Cells were used between the fourth and tenth passages. The human NCI-H460 lung carcinoma cells (ATCC HTB 177) were cultured in RPMI-1640 supplemented with 10% FCS. DMEM and RPMI-1640 were purchased from SIGMA (Milan, Italy), trypsin ethylenediamine tetraacetate, penicillin (10.000 U/mL), streptomycin (10 mg/mL), tricine buffer (1 M, pH 7.4), non-essential amino acid solution (100×), and fetal calf serum (FCS) were purchased from Invitrogen (Carlsbad, CA, USA). Disposable culture flasks and Petri dishes are from Corning Glassworks (Corning, NY).

#### 6.2.2. Cell proliferation assay

Rat SMCs were seeded at a density of $2 \times 10^5$ cells/Petri dish (35 mm) and incubated with DMEM supplemented with 10% FCS. Twenty-four hours later, the medium was changed to one containing 0.4% FCS to stop cell growth, and the cultures were incubated for 72 h. At this time (time 0), the medium was replaced with one containing 10% FCS in the presence or absence of known

concentrations of the tested compounds, and the incubation was continued for a further 72 h at 37 °C. NCIH460 cells were seeded at a density of $8 \times 10^4$ cells/Petri dish (35 mm), and incubated with RPMI-1640 supplemented with 10% FCS. Twenty-four hours after seeding, cells were exposed to test compound, then harvested 72 h later. Cell proliferation was evaluated by cell counting after trypsinization of the monolayers with use of a Coulter Counter model ZM.[34] All the compounds were dissolved in DMSO prior to dilution, being the final concentration of DMSO at a maximum of 1%. The concentration of compounds required to inhibit 50% of cell proliferation ($IC_{50}$) was calculated by linear regression analysis of the logarithm of the concentration (in micromoles per liter) versus logit.

#### 6.2.3. DNA topoisomerase II activity assay

For the assay the supercoiled pRYG DNA was utilized as substrate according to protocol provided by TopoGen Inc. (Columbus, USA). Supercoiled pRYG DNA was incubated in a reaction buffer containing 10 mM Tris–HCl, pH 7.9, 1 mM EDTA, 150 mM NaCl, 0.1% BSA, 0.1 mM spermidine, and 5% glycerol in the presence of two units of DNA toposiomerase II. The tested compounds were added at the indicated concentrations and after 10 min at 37 °C the reaction was stopped by addition of the stop buffer containing the loading dye (15 sarkosyl, 0.025% bromophenol blue, 5% glycerol). Then the reaction mixture was analyzed on a 1% agarose gel by running at 80 V in TAE buffer (400 mM Tris–base, 10 mM EDTA, 200 mM sodium acetate, pH 8.3). Gels were stained with ethidium bromide and the image acquired with Gel Doc acquisition system and Quantity One software (Bio-Rad). The analysis of the DNA intercalating activity of the tested compounds were carried out under the same experimental condition in the absence of the DNA toposiomerase II.

#### 6.2.4. Cell cycle analysis

Flow cytometry was utilized to analyze cell cycle distribution. Cells were trypsinized and centrifuged for 5 min at 1.000 rpm. Pellets were fixed with 62% ethanol, then resuspended in 0.4 mL of staining buffer of propidium iodide (10 μg/mL RNAse, 1% NP-40, 5 μg/ml propidium iodide, in $H_20$). Samples were placed in the dark for 30 min and the fluorescence of individual nuclei was measured. Nuclear propidium Iodide fluorescence signal was recorded on the FL3 channel of a FACS scan flow cytometer (Becton Dickinson). The number of cells in G0/G1, S and G2/M phases was expressed as percentages of total events (10.000 cells).[35]

#### 6.2.5. In vivo antitumoral evaluation

The study was carried out using female athymic Swiss nude mice, 8–10 weeks old (Charles River, Calco, Italy). Mice were kept in aminar flow rooms at constant temperature and humidity with free access to food and water. Experimental protocols were approved by the Ethics Committee for Animal Experimentation of the Istituto Nazionale Tumori, Milan, according to the United Kingdom Coordinating Committee on Cancer Research Guidelines.[36]

The human lung carcinoma NCI-H460 was maintained in vivo by serial s.c. passages of tumor fragments (about $2 \times 2 \times 6$ mm) in healthy mice, as described previously.[37] The experimental groups included 4–5 mice bearing bilateral s.c. tumors. Tumor fragments were implanted on day 0, and tumor growth was followed by biweekly measurements of tumor diameters with a Vernier caliper. Tumor weight (TW) was calculated according to the formula: TW (mg) = tumor volume ($mm^3$) = $d^2 \times D/2$ where $d$ and $D$ are the shortest and the longest diameter, respectively. Treatment started at day 2, when TW was around 50 mg. Compound **11a** was dissolved in DMSO to a final concentration of 10% in sterile water, and was delivered iv according to a every 4th day schedule (q4d) for four times. For statistical analysis, TW was compared in treated versus control mice by unpaired Student's *t*-test (two-tailed).

### 6.3. NMR experiments

#### 6.3.1. Sample preparation

The oligonucleotide 5′-d(CGGCCG)-3′ was purchased as sodium salt from Roche Diagnostics (Monza, Italy) and utilized without further purification. It was dissolved in $D_2O$ (99.9% isotopic purity, Isotec, USA) at 2 mM concentration, in the presence of 0.025 M NaCl. pH values were corrected to 5.5 by adding small amounts of 1 mM NaOD or 1 mM DCl solutions. The trifluoroacetate salt of **11a** was prepared by dissolving 1 mg of the free base in trifluoroethanol (TFE, Sigma–Aldrich, Milano, Italy) and adding two equivalents of trifluoroacetic acid dissolved in TFE. The mixture was taken to dryness under vacuum. The obtained trifluoroacetate salt was dissolved in $D_2O$ 99.9%, in the presence of NaCl 25 mM. The pH value of the solution was adjusted to 5.5 as described above. The final concentration was 0.3 mM, as checked with a calibrated external reference.

#### 6.3.2. NMR experiments

The NMR spectra were recorded on a Bruker AV600 spectrometer operating at 600.10 MHz (proton frequency). Chemical shifts ($\delta$) are measured in ppm, with $^1H$ spectra referenced to external DSS (2,2-dimethyl-2-silapentane-5-sulfonate sodium salt) set at 0.00 ppm. Estimated accuracy is within 0.03 ppm. Titration experiments were performed by adding increasing amounts of oligonucleotide stock solutions to **11a**–trifluoroacetate dissolved in $D_2O$.

Phase sensitive NOESY spectra were acquired at temperatures ranging from 5 °C to 25 °C in TPPI (Time Proportional Phase Increments) mode, with $640 \times 4$ K complex FIDs, spectral width of 8400 Hz, recycling delay of 1.3 s, 80 scans. Mixing times ranged from 50 ms to 300 ms. TOCSY spectra were acquired with the use of MLEV-17 spin-lock pulse (field strength 10.000 Hz, 20–80 ms total duration). For samples dissolved in $D_2O$, water suppression was achieved by pre-saturation, placing the carrier frequency on the HDO resonance. All spectra were transformed and weighted with a 90° shifted sine-bell squared function to $2\ K \times 2\ K$ real data points.

Proton assignments for **11a**, both free and in the complex with $d(CGGCCG)_2$, were accomplished by means of standard two-dimensional homonuclear correlation techniques. Protons residing on the *N*-methyl pyrrole moiety were assigned by means of the observed NOE interactions with the methyl groups, resonating at 3.17 and 3.58 ppm, and by the vicinal coupling constant values, measured on resolution-enhanced spectra ($^3J_{4,5}$ = 2.6 Hz; $^3J_{2,3}$ = 1.9 Hz). The $^1H$ NMR sequential assignments of $d(CGGCCG)_2$ with and without ligand were performed by applying well established procedures for the analysis of double-stranded type B-DNA.[38] Spectral manipulation and analysis were performed respectively with TOPSPIN (v. 1.3, Bruker Biospin, Rheinstetten, Germany) and SPARKY.[39]

### 6.4. Molecular modeling

Using the PDB structure 1CX3 as a template, molecular models were built with the MOE software package[40] and compound **11a** was manually docked in the DNA double strand. A total of six models were prepared according to all the possible relative orientations of the heterocyclic moieties within either the major and the minor groove. All models were subjected to a preliminary geometry optimization (rmsd = 0.1) using the default MMFF94x force field, the default distance dependent solvation model for water and by keeping a positional restraints on DNA heavy atoms of 10 kcal/mol. AM1-BCC partial atomic charges compatible with the General Amber Force Field (*gaff*)[41] were calculated for compound **11a** using

the *antechamber* module implemented in the Amber9 suite.[42,43] A topological file and a coordinate set was prepared for the complex using the *leap* module of the Amber9 package accordingly to the *ff03* and *gaff* force fields.[44,45] The complex was solvated by placing a periodic box of TIP3P water up to a distance of 10 Å from the DNA complex (total vdW box size: 53.0 Å × 50.9 Å × 50.1 Å), and the system was neutralized by adding $Na^+$ ions. After a careful equilibration of the water box, the full system was gently heated through six 5 ps molecular dynamic (MD) runs where phosphate backbone restraints were gradually reduced from 10 to 5 kcal/mol, while the temperature was raised from 0 to 300 K. The heating was followed by a 100 ps run in NVT ensemble and four 100 ps run in NPT ensemble where backbone restraints were gradually reduced from 5 to 0 kcal/mol. Finally, 8 ns NPT production runs were performed at 300 K without any restraints, with the exception of bonds involving hydrogen atoms which were constrained through the SHAKE algorithm.[46] A time step of 0.002 ps was used and frames were saved every 500 steps (1 frame/ps). Resulting trajectories were post-processed using the MM-PBSA approach in order to estimate relative energies of binding.[47] Trajectory analysis were performed with the *ptraj* module of the Amber9 package. Molecular graphics images were produced with either MOE or the UCSF Chimera package.[48]

## Acknowledgments

We thank MIUR for financial support (Grants COFIN and FIRB). Alessandro Contini is grateful to the Centro Interunivesitario Lombardo per l'Elaborazione Automatica (CILEA) for computational facilities.

## Supplementary data

Supplementary data associated (NMR details and extended tables, further computational details, spectroscopic and analytical data for compounds **7a**–**h**, **9**, **11a**–**c**) with this article can be found, in the online version, at doi:10.1016/j.bmc.2011.08.016.

## References and notes

1. Braña, M. F.; Castellano, J. M.; Morán, M.; Pérez de Vega, M. J.; Romerdahl, C. R.; Qian, X.-D.; Bousquet, P.; Emling, F.; Schlick, E.; Keilhauer, G. *Anti-Cancer Drug Des.* **1993**, *8*, 257.
2. Braña, M. F.; Castellano, J. M.; Morán, M.; Pérez de Vega, M. J.; Perron, D.; Conlon, D.; Bousquet, P. F.; Romerdahl, C. A.; Robinson, S. P. *Anti-Cancer Drug Des.* **1996**, *11*, 297.
3. Braña, M. F.; Cacho, M.; Gradillas, A.; de Pascual-Teresa, B.; Ramos, A. *Curr. Pharm. Des.* **2001**, *7*, 1745.
4. Bousquet, P. F.; Brana, M. F.; Conlon, D.; Fitzgerald, K. M.; Perron, D.; Cocchiaro, C.; Miller, R.; Moran, M.; George, J.; Qian, X. -D. *Cancer Res.* **1995**, *55*, 1176.
5. McRipley, R. J.; Burns-Horwitz, P. E.; Czerniak, P. M.; Diamond, R. J.; Diamond, M. A.; Miller, J. L. D.; Page, F. J.; Dexter, D. L.; Chen, S. F. *Cancer Res.* **1994**, *54*, 159.
6. Nitiss, J. L.; Zhou, J. F.; Rose, A.; Hsiung, Y. C.; Gale, K. C.; Osheroff, N. *Biochemistry* **1998**, *37*, 3078.
7. Viergutz, W.; Koser, S. Preparation of aromatic bisimides from anhydrides. Ger. Offen. **1998**, WXXBX DE 19720803 A1 19981119. *Chem: Abstr.* **1998**, *130*, 24969.
8. Braña, M. F.; Castellano, J. M.; Perron, D.; Maher, C.; Conlon, D.; Bosquet, P. F.; George, J.; Qian, X.-D.; Robinson, S. P. *J. Med. Chem.* **1997**, *40*, 449.
9. Hernandez, L.; Cholody, W. M.; Hudson, E. A.; Resau, J. H.; Pauly, G.; Michejda, C. J. *Cancer Res.* **1995**, *55*, 2338.
10. Cholody, W. M.; Hernandez, L.; Hassner, L.; Scudiero, D. A.; Djurickovic, D. B.; Michejda, C. J. *J. Med. Chem.* **1995**, *38*, 3043.
11. Leng, F. F.; Priebe, W.; Chaires, J. B. *Biochemistry* **1998**, *37*, 1743.
12. Chaires, J. B.; Leng, F. F.; Przewloka, T.; Fokt, I.; Ling, Y. H.; Perez-soler, R.; Priebe, W. *J. Med. Chem.* **1997**, *40*, 261.
13. Gamage, S. A.; Spicer, J. A.; Atwell, G. J.; Finlay, G. J.; Baguley, B. C.; Denny, W. A. *J. Med. Chem.* **1999**, *42*, 2383.
14. Gamage, S. A.; Spicer, J. A.; Finlay, G. J.; Stewart, A.; Charlton, P.; Baguley, B. C.; Denny, W. A. *J. Med. Chem.* **2001**, *44*, 1407.
15. Spicer, J. A.; Gamage, S. A.; Rewcastle, G. W.; Finlay, G. J.; Baguley, B. C.; Denny, W. A. *J. Med. Chem.* **2000**, *43*, 1350.
16. Marminon, C.; Facompre, M.; Bailly, C.; Hickman, J.; Pierre, A.; Pfeiffer, B.; Renard, P.; Prudhomme, M. *Eur. J. Med. Chem.* **2002**, *37*, 435.
17. Hasinoff, B. B.; Zhang, R.; Wu, X.; Guziec, L. J.; Guziec, F. S.; Marshall, K.; Yalowich, J. C. *Bioorg. Med. Chem.* **2009**, *17*, 4575.
18. Cherney, R. J.; Swartz, S. G.; Patten, A. D.; Akamike, E.; Sun, J. H.; Kaltenbach, R. F.; Seitz, S. P.; Behrens, C. H.; Getahun, Z.; Trainor, G. L.; Vavala, M.; Kirshenbaum, M. R.; Papp, L. M.; Stafford, M. P.; Czerniak, P. M.; Diamond, R. J.; McRipley, R. J.; Page, R. J.; Gross, J. L. *Bioorg. Med. Chem. Lett.* **1997**, *7*, 163.
19. Lavielle, G.; Hautefaye, P.; Atassi, G.; Pierre, A.; Kraus-Berthier, L.; Leonce, S. Preparation of bis(imide) derivatives and their pharmaceutical compositions which are useful as anticancer agents. Eur. Pat. Appl. 1998, EPXXDW EP 820985 19980128. *Chem. Abstr.* **1998**, *128*, 153998.
20. Gazzard, L. J.; Ha, E. H.; Jackson, D. Y.; Um, J. M. Preparation of heterocyclyl bis-1,8-naphthalimide compounds as antibody drug conjugates. U.S. Pat. Appl. Publ. 2006 part of U.S. Ser. No. 311,591. USXXCO US 2006182751 A1 20060817. *Chem. Abstr.* **2006**, *145*, 249519.
21. Braña, M. F.; Cacho, M.; Garcia, M. A.; de Pascual-Teresa, B.; Ramos, A.; Dominguez, M. T.; Pozuelo, J. M.; Abradelo, C.; Rey-Stolle, M. F.; Yuste, M.; Banez-Coronel, M.; Lacal, J. C. *J. Med. Chem.* **2004**, *47*, 1391.
22. Braña, M. F.; Cacho, M.; Ramos, A.; Dominguez, M. T.; Pozuelo, J. M.; Abradelo, C.; Rey-Stolle, M. F.; Yuste, M.; Carrasco, C.; Bailly, C. *Org. Biomol. Chem.* **2003**, *1*, 648.
23. Braña, M. F.; Cacho, M.; Garcia, M. A.; de Pascual-Teresa, B.; Ramos, A.; Acero, N.; Llinares, F.; Munoz-Mingarro, D.; Abradelo, C.; Rey-Stolle, M. F.; Yuste, M. *J. Med. Chem.* **2002**, *45*, 5813.
24. Carrasco, C.; Joubert, A.; Tardy, C.; Maestre, N.; Cacho, M.; Braña, M. F.; Bailly, C. *Biochemistry* **2003**, *42*, 11751.
25. Bailly, C.; Carrasco, C.; Joubert, A.; Bal, C.; Wattez, N.; Hildebrand, M. -P.; Lansiaux, A.; Colson, P.; Houssier, C.; Cacho, M.; Ramos, A.; Braña, M. F. *Biochemistry* **2003**, *42*, 4136.
26. Braña, M. F.; Gradillas, A.; Gomez, A.; Acero, N.; Llinares, F.; Munoz-Mingarro, D.; Abradelo, C.; Rey-Stolle, F.; Yuste, M.; Campos, J.; Gallo, M. A.; Espinosa, A. *J. Med. Chem.* **2004**, *47*, 2236.
27. Ferri, N.; Beccalli, E. M.; Contini, A.; Corsini, A.; Antonino, M.; Radice, T.; Pratesi, G.; Tinelli, S.; Zunino, F.; Gelmi, M. L. *Bioorg. Med. Chem.* **2008**, *16*, 1691.
28. Gallego, J.; Reid, B. R. *Biochemistry* **1999**, *38*, 15104.
29. Gallego, J. *Nucl. Acids Res.* **2004**, *32*, 3607.
30. Wang, J.; Morin, P.; Wang, W.; Kollman, P. A. *J. Am. Chem. Soc.* **2001**, *133*, 5221.
31. Ferri, N.; Corsini, A.; Bottino, P.; Clerici, F.; Contini, A. *J. Med. Chem.* **2009**, *52*, 4087.
32. Beccalli, E. M.; Gelmi, M. L.; Marchesini, A. *Eur. J. Org. Chem.* **1999**, 1421.
33. Jeanes, A.; Adams, R. *J. Am. Chem. Soc.* **1937**, *59*, 2608.
34. Corsini, A.; Mazzotti, M.; Raiteri, M.; Soma, M. R.; Gabbiani, G.; Fumagalli, R.; Paoletti, R. *Atherosclerosis* **1993**, *101*, 117.
35. Ferri, N.; Yokoyama, K.; Sadilek, M.; Paoletti, R.; Apitz-Castro, R.; Gelb, M. H.; Corsini, A. *Br. J. Pharmacol.* **2003**, *138*, 811.
36. Mbidde, E. K.; Selby, P. J.; Perren, T. J.; Dearnaley, D. P.; Whitton, A.; Ashley, S.; Workman, P.; Bloom, H. J.; McElwain, T. J. *Br. J. Pharmacol.* **1988**, *58*, 779.
37. Pratesi, G.; Manzotti, C.; Tortoreto, M.; Prosperi, E.; Zunino, F. *Tumori* **1989**, *75*, 60.
38. Wüthrich, K. *NMR of Proteins and Nucleic Acids*; Wiley: New York, 1986.
39. Goddard, T. D.; Kneller, D. G. SPARKY 3, University of California, San Francisco, USA, http://www.cgl.ucsf.edu/home/sparky/.
40. MOE v 2009.10, Chemical Computing Group, Montreal, Canada, http://www.chemcomp.com.
41. Wang, J.; Wolf, R. M.; Caldwell, J. W.; Kollman, P. A.; Case, D. A. *J. Comput. Chem.* **2004**, *25*, 1157.
42. Case, D. A.; Cheatham, T. E., 3rd; Darden, T.; Gohlke, H.; Luo, R.; Merz, K. M., Jr.; Onufriev, A.; Simmerling, C.; Wang, B.; Woods, R. J. *J. Comput. Chem.* **2005**, *26*, 1668.
43. Case, D. A.; Darden, T. A.; Cheatham, T. E. I.; Simmerling, C. L.; Wang, J.; Duke, R. E.; Luo, R.; Merz, K. M., Jr.; Pearlman, D. A.; Crowley, M.; Walker, R. C.; Zhang, W.; Wang, B.; Hayik, S.; Roitberg, A.; Seabra, G.; Wong, K. F.; Paesani, F.; Wu, X.; Brozell, S.; Tsui, V.; Gohlke, H.; Yang, L.; Tan, C.; Mongan, J.; Hornak, V.; Cui, G.; Beroza, P.; Mathews, D. H.; Schafmeister, C.; Ross, W. S.; Kollman, P. A. *AMBER 9*; University of California: San Francisco, 2006.
44. Duan, Y.; Wu, C.; Chowdhury, S.; Lee, M. C.; Xiong, G.; Zhang, W.; Yang, R.; Cieplak, P.; Luo, R.; Lee, T.; Caldwell, J.; Wang, J.; Kollman, P. A. *J. Comput. Chem.* **2003**, *24*, 1999.
45. Lee, M. C.; Duan, Y. *Proteins* **2004**, *55*, 620.
46. Ryckaert, J. P.; Ciccotti, G.; Berendsen, H. J. C. *J. Comput. Phys.* **1977**, *23*, 327.
47. Srinivasan, J.; Cheatham, T.; Cieplak, P.; Kollman, P. A.; Case, D. A. *J. Am. Chem. Soc.* **1998**, *120*, 9401.
48. Pettersen, E. F.; Goddard, T. D.; Huang, C. C.; Couch, G. S.; Greenblatt, D. M.; Meng, E. C.; Ferrin, T. E. *J. Comput. Chem.* **2004**, *25*, 1605.